

Appendix

A Summary of Notations

We summarize the notations used in this paper in Tab. 2.

B Additional Experiments and Details

We provide the exact number of images in the initial labeled set \mathcal{L} and the query set \mathcal{Q} for each rare slice experiment in Tab. 3. Further, in Fig. 10 and Fig. 11 we qualitatively show how TALISMAN is able to fix a false negative motorcycle failure case. Lastly, in Fig. B we show the effectiveness of TALISMAN in another rare classes scenario on the BDD100K dataset. We observe that SMI functions used in TALISMAN outperform the baselines by $\approx 8\% - 14\%$ AP of the rare class and by $\approx 3\% - 4\%$ in terms of the mAP.



Fig. 10: A false negative motorcycle at night on the road (left) fixed to a true positive detection (right) using TALISMAN.

Topic	Notation	Explanation
TALISMAN (Sec. 4)	\mathcal{U}	Unlabeled set of $ \mathcal{U} $ instances
	\mathcal{A}	A subset of \mathcal{U}
	S_{ij}	Similarity between any two data points i and j
	f	A submodular functions
	\mathcal{L}	Labeled set of data points
	\mathcal{Q}	Query set
	\mathcal{M}	Object detection model
	B	Active learning selection budget
	\mathcal{I}_q	A single query image in the query set \mathcal{Q}
	\mathcal{I}_u	A single unlabeled image in the unlabeled set \mathcal{U}
	T	Number of region of interests (RoIs) in a single query image \mathcal{I}_q
	P	Number of proposals in a single unlabeled image \mathcal{I}_u
	\mathcal{E}_q	Embedding of T RoIs in \mathcal{I}_q , $\mathcal{E}_q \in \mathbb{R}^{T \times D}$
	\mathcal{E}_u	Embedding of P proposals in \mathcal{I}_u , $\mathcal{E}_u \in \mathbb{R}^{P \times D}$
	D	Dimensionality of each feature vector representing a RoI/proposal
	F_θ	Feature extraction module with parameters θ
	\mathcal{X}_{qu}	Intermediate score map obtained by computing cosine similarity between \mathcal{E}_q and \mathcal{E}_u , $\mathcal{X}_{qu} \in \mathbb{R}^{T \times P}$
TALISMAN for Rare Classes (Sec. 5.3)	$\mathcal{C}_i^{\mathcal{L}}$	Number of objects in \mathcal{L} that belong to the rare (infrequent) class i . The total number of rare objects in \mathcal{L} is $ \mathcal{C}^{\mathcal{L}} $
	$\mathcal{B}_j^{\mathcal{L}}$	Number of objects in \mathcal{L} that belong to the frequent class j . The total number of rare objects in \mathcal{L} is $ \mathcal{B}^{\mathcal{L}} $
	ρ	Imbalance ratio between $\mathcal{C}_i^{\mathcal{L}}$ and $\mathcal{B}_j^{\mathcal{L}}$
TALISMAN for Rare Slices (Sec. 5.4)	$ \mathcal{O}_c^A $	Total number of objects in \mathcal{L} that belong to class c and <i>have</i> the attribute A
	$ \mathcal{O}_c^{\tilde{A}} $	Total number of objects in \mathcal{L} that belong to class c and <i>do not have</i> the attribute A
	ρ	Imbalance ratio between $ \mathcal{O}_c^A $ and $ \mathcal{O}_c^{\tilde{A}} $

Table 2: Summary of notations used throughout this paper

Table 3: Number of data points in the initial labeled set \mathcal{L} and query set \mathcal{Q} for different rare slice experiments in Sec. 5.4

Rare Slice	Initial \mathcal{L} Size (# Images)	Query Set \mathcal{Q} Size (# Images)
Motorcycle at Nighttime	363	5
Bicycle at Nighttime	348	5
Pedestrian at Nighttime	355	3
Pedestrian in Rainy Weather	361	5
Pedestrian on a Highway	362	5

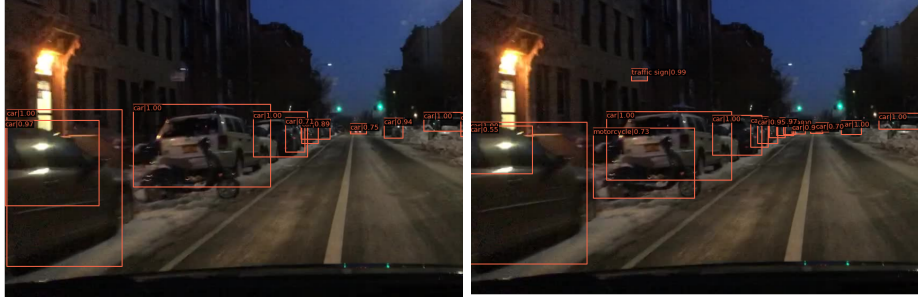


Fig. 11: A false negative motorcycle at night parked on the road (left) fixed to a true positive detection (right) using TALISMAN.

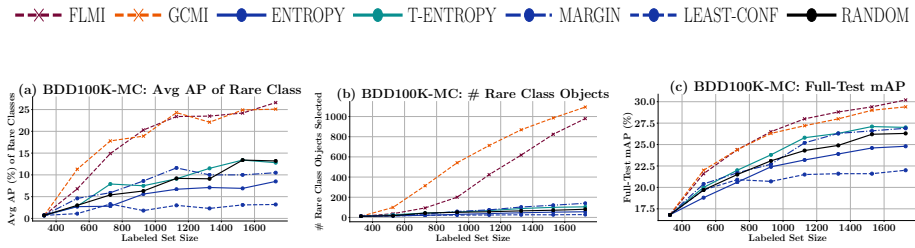


Fig. 12: Active Learning with Motorcycle (MC) rare class on BDD100K. Left side plot (a) shows the AP of the rare class, center plot (b) show the number of objects selected that belong to the rare class, and right side plots (c) show the mAP on the full test set of BDD100K. We observe that the SMI functions (FLMI, GCMI) outperform other baselines by $\approx 8\% - 14\%$ AP of the rare class.